Propagating bound states in the continuum at the surface of a photonic crystal

ZHEN HU[1,*] AND YA YAN LU[2]

[1] Department of Mathematics, Hohai University, Nanjing, Jiangsu, China
[2] Department of Mathematics, City University of Hong Kong, Kowloon, Hong Kong
[*] Corresponding author: huzhen1230@gmail.com

Compiled July 18, 2017

Bound states in the continuum (BICs) are trapped or guided modes with their frequencies within the radiation continuum. On periodic structures, BICs have interesting properties and potentially important applications. It is known that BICs can exist at the surface of a photonic crystal (PhC), and they are distinctively different from the well-known surface Bloch modes below the lightline. However, for a given structure with specific geometric and material parameters, it is difficult to predict whether BICs exist or not. In this paper, using an efficient computational method, we calculate BICs at the surface of a two dimensional PhC consisting of dielectric rods, and determine the existence domain in the plane of the refractive index and the radius of the surface rods. The boundary of the existence domain reveals that the BICs cease to exist when the bulk PhC can no longer confine light. In addition, the frequency and wavenumber of the BIC can approach the lightline, leading to bound states on the lightline and special highly confined surface Bloch modes below the lightline.

OCIS codes: *(240.6690) Surface waves; (050.5298) Photonic crystals; (130.2790) Guided waves; (050.1755) Computational electromagnetic methods.*

http://dx.doi.org/

1. INTRODUCTION

Optical bound states in the continuum (BICs) have recently attracted much attention [1]. The concept of BIC was originally developed in quantum mechanics [2]. For classical waves, a BIC is a trapped or guided mode with a frequency in the frequency interval where outgoing radiation modes exist. In the simplest setting, a BIC is trapped mode around a local distortion in a waveguide, and it exists at a frequency for which the waveguide still has propagating modes [3–8]. A BIC can also be a special guided mode of a z-invariant waveguide (z is the waveguide axis), where waves can also propagate away in the transverse direction through a lateral structure [9–12]. On periodic structures surrounded by homogeneous media, a BIC can be a standing wave or a propagating Bloch mode with a frequency such that propagating waves with compatible periodicity exist in the surrounding media [13–30]. Some BICs having incompatible symmetry with the outgoing waves [13–19]. They are often labeled as symmetry-protected BICs, and their existence can be rigorously proved [6, 13, 17, 19]. There are also BICs without apparent symmetry incompatibility with the radiation modes [20–30]. Some physical arguments and mathematical models have been used to explain the appearance of these BICs without symmetry protection [23, 31, 32].

The BICs on periodic structures have interesting properties and potentially important applications [1]. For incident waves impinging on a periodic structure with a BIC, the transmission and reflection coefficients are discontinuous at the frequency and wavevector of the BIC, and exhibit arbitrarily close total transmissions and total reflections [33, 34]. For incident waves of fixed frequency and wavevector, the transmission and reflections coefficients are also discontinuous at the geometric and material parameters of the BIC [30]. These properties can be explored in filtering, sensing and switching applications. The BICs are related to the nonuniqueness of related boundary value problems with given incident waves [13], and they give rise to multiple solutions for weak incident waves when the structure contains nonlinear media [35], and the multiple solutions have potential applications in optical switching. Furthermore, near BICs on periodic structures, there are continuous families of resonant modes with quality factors approaching infinity. The strong resonances can be used to enhance nonlinear optical effects [36], quantum optical effects, and other emission processes. In particular, light confinement related to BICs has been used to design a compact laser that emits a high-quality beam [37]. Moreover, some BICs related to separability have interesting properties that can be used to control the direction and the dimension of the radiated field [38].

It is desirable to develop a better understanding for those BICs without symmetry protection. In many cases [20–22, 24, 25, 28, 30], the periodic structures are sandwiched between two identical homogeneous media, and are symmetric with respect to the mid-plane parallel to the periodic directions. The structure studied by Hsu *et al.* in [23] does not have this reflection symmetry. A BIC is found along the surface of a semi-infinite two-dimension (2D) photonic crystal (PhC), where the PhC is a square lattice of dielectric rods surrounded by air, and the array at the surface contains rods with a larger radius [23]. Guided modes at the surface of a PhC are well known [39–41], but they usually exist below the lightline, i.e., $k_0 < |\beta|$, where k_0 is the free space wavenumber and β is the Bloch wavenumber of the mode. In contrast, the BIC is above the lightline, i.e., $k_0 > |\beta|$. In [23], a temporal coupled mode model is developed to explain the appearance of the BIC, but it is still not clear why the BIC exists for some parameter values and does not exist for other parameter values.

In this paper, we perform an extensive numerical study for BICs at the surface of a 2D PhC, and determine the domain of existence in the plane of two parameters: the radius and dielectric constant of the rods in the surface array. The boundary of the domain reveals that the BICs cease to exist when the PhC can no longer confine the wave or when the frequency and Bloch wavenumber reach the lightline. We also determine a domain in the frequency and wavenumber plane for the corresponding values of the BICs, and demonstrate a close relation with the projected band structure of the PhC. Our results are obtained using a highly efficient special computational method and an accurate boundary truncation technique that terminates the semi-infinite PhC. The method works well even when the wave field decays very slowly in the PhC.

2. FORMULATION AND COMPUTATION METHOD

In Fig. 1, we show a 2D semi-infinite PhC structure consisting of

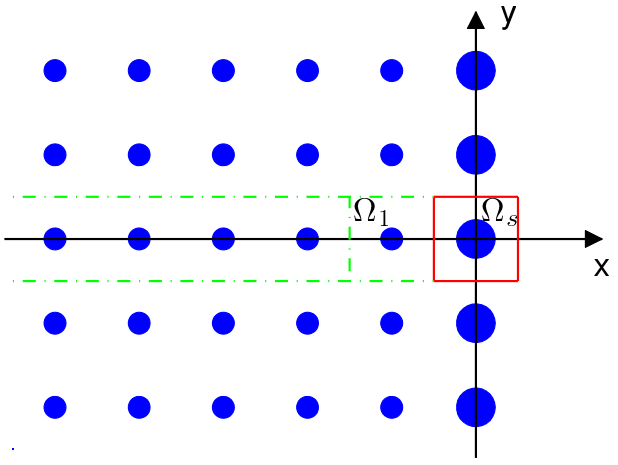

Fig. 1. A 2D semi-infinite PhC structure consisting of dielectric rods on a square lattice. The rods are parallel to the z axis and surrounded by air. The array along the y axis corresponds to the surface of the structure.

circular dielectric rods on a square lattice with lattice constant a. The dielectric rods are infinitely long, surrounded by air, and parallel to the z axis, where $\{x, y, z\}$ is a Cartesian coordinate system. The regular rods with their centers located in the left half of the xy plane, have radius r_1 and dielectric constant ϵ_1. The rods in the surface array (with their centers located on the y axis) have radius r_s and dielectric constant ϵ_s which in general are different from r_1 and ϵ_1. Clearly, the structure is invariant in z and periodic in y with period a.

For the E-polarization, the governing equation is the Helmholtz equation

$$\frac{\partial^2 u}{\partial x^2} + \frac{\partial^2 u}{\partial y^2} + k_0^2 \epsilon\, u = 0, \tag{1}$$

where u is the z component of the electric field, $k_0 = \omega/c$ is the free space wavenumber, ω is the angular frequency, c is the speed of light in vacuum, and $\epsilon = \epsilon(x, y)$ is the real dielectric function. A Bloch surface mode on this structure is a non-zero solution of Eq. (1) given by

$$u(x, y) = \phi(x, y) e^{i\beta y}, \tag{2}$$

where β is the real Bloch wavenumber, ϕ is periodic in y with period a, and $u \to 0$ as $x \to \pm\infty$. This surface mode is a BIC when k_0 and β satisfy the condition $k_0 > |\beta|$.

The above gives rise to an eigenvalue problem defined on one period of the structure, i.e., the 2D domain given by $-\infty < x < \infty$ and $-a/2 < y < a/2$. Since two parameters ω and β are involved, one of them can be specified and the other can be determined as the eigenvalue. This approach is inefficient, since the differential equation must be discretized on the 2D domain and either ω or β must be continuously scanned. In the following, we present an efficient method that reformulates the eigenvalue problem on two line segments of length a, and further approximates the problem by a system of two real equations for ω and β. The system can be solved by standard root-finding methods.

To reformulate the eigenvalue problem on two line segments, we need to define three basic operators $\mathcal{P}$, $\mathcal{L}$ and Λ. They depend on ω and β, and can be approximated by small matrices when ω and β are given. The operator $\mathcal{P}$ satisfies

$$\frac{\partial u}{\partial x} = \mathcal{P} u \quad \text{at} \quad x = \frac{a}{2}, \tag{3}$$

and it can be use to get rid of the free space in the right from the computation domain. This operator appears in the rigorous mathematical formulation of diffraction grating problems. It is well-known that for $x > r_s$, u can be expanded in propagating and evanescent plane waves:

$$u(x, y) = \sum_{m=-\infty}^{\infty} c_m e^{i(\beta_m y + \gamma_m x)}, \quad x > r_s, \tag{4}$$

where $\beta_m = \beta + 2\pi m/a$, $\gamma_m = (k_0^2 - \beta_m^2)^{1/2}$, and c_m are expansion coefficients. The operator $\mathcal{P}$ is defined as a linear operator satisfying

$$\mathcal{P} e^{i\beta_m y} = i\gamma_m e^{i\beta_m y}, \quad m = 0, \pm 1, \pm 2, \ldots \tag{5}$$

By comparing u and $\partial u/\partial x$ at $x = a/2$ and using the linearity of $\mathcal{P}$, Eq. (3) can be obtained.

Similarly, the operator $\mathcal{L}$ allows us to remove the bulk PhC in the left from the computation domain. It satisfies

$$\frac{\partial u}{\partial x} = \mathcal{L} u \quad \text{at} \quad x = -\frac{a}{2}. \tag{6}$$

Unfortunately, $\mathcal{L}$ can not be explicitly written down. Instead of the simple plane wave expansion (4), in the PhC, u can be expanded in Bloch modes, that is

$$u(x,y) = \sum_{j=1}^{\infty} b_j \psi_j(x,y) e^{i(\beta y - \alpha_j x)}, \quad x < -\frac{a}{2}, \tag{7}$$

where ψ_j is periodic in both x and y with period a, and b_j is the expansion coefficient. The Bloch wavenumber α_j is complex with a positive imaginary part, so that $u \to 0$ as $x \to -\infty$. Equation (6) is derived from the above expansion following a procedure developed in our earlier work for truncating PhC waveguides [42]. A brief summary is given in Appendix A.

The operator Λ is the so-called Dirichlet-to-Neumann (DtN) map for Helmholtz equation (1) on square Ω_s given by $|x| < a/2$ and $|y| < a/2$, and shown in Fig. 1. To simplify the notations, we let $x_j = (1/2 - j)a$ and $y_k = (1/2 - k)a$, denote u and $\partial_x u$ on vertical edges at x_j by u_j and $\partial_x u_j$, respectively; and denote u and $\partial_y u$ on horizontal edges at y_k by v_k and $\partial_y v_k$, respectively. For any u satisfying Eq. (1) in Ω_s, the operator Λ gives

$$\Lambda \begin{bmatrix} v_0 \\ u_1 \\ u_0 \\ v_1 \end{bmatrix} = \begin{bmatrix} \partial_y v_0 \\ \partial_x u_1 \\ \partial_x u_0 \\ \partial_y v_1 \end{bmatrix}, \tag{8}$$

where u_0, u_1, v_0 and v_1 and their derivatives are restricted to the boundary of Ω_s, i.e., for $|x| < a/2$ or $|y| < a/2$ only. Notice that Λ maps u to its normal derivative on the boundary of Ω_s. The DtN maps are useful for analyzing periodic structures such as PhCs, since they are identical for all unit cells with the same dielectric function, and they can be used to avoid duplicated calculations. For unit cells with circular cylinders, Λ can be approximated by a small matrix based on expansions in cylindrical waves [42–44].

Since we are looking for a Bloch mode given in Eq. (2), u satisfies the following quasi-periodic conditions

$$v_0 = v_1 e^{i\beta a}, \quad \partial_y v_0 = \partial_y v_1 \, e^{i\beta a}. \tag{9}$$

From Eqs. (8) and (9), we can eliminate v_0, v_1 and their derivatives, and find the operator $\mathcal{M}$ satisfying

$$\mathcal{M} \begin{bmatrix} u_1 \\ u_0 \end{bmatrix} = \begin{bmatrix} \mathcal{M}_{11} & \mathcal{M}_{12} \\ \mathcal{M}_{21} & \mathcal{M}_{22} \end{bmatrix} \begin{bmatrix} u_1 \\ u_0 \end{bmatrix} = \begin{bmatrix} \partial_x u_1 \\ \partial_x u_0 \end{bmatrix}, \tag{10}$$

where $\mathcal{M}$ is also given in 2×2 blocks.

From Eqs. (3), (6) and (10), we obtain

$$\mathcal{A} \begin{bmatrix} u_1 \\ u_0 \end{bmatrix} = \begin{bmatrix} \mathcal{A}_{11} & \mathcal{A}_{12} \\ \mathcal{A}_{21} & \mathcal{A}_{22} \end{bmatrix} \begin{bmatrix} u_1 \\ u_0 \end{bmatrix} = 0, \tag{11}$$

where $\mathcal{A}_{11} = \mathcal{M}_{11} - \mathcal{L}$, $\mathcal{A}_{12} = \mathcal{M}_{12}$, $\mathcal{A}_{21} = \mathcal{M}_{21}$ and $\mathcal{A}_{22} = \mathcal{M}_{22} - \mathcal{P}$. Notice that Λ depends on ω, $\mathcal{M}$, $\mathcal{L}$, $\mathcal{P}$ and $\mathcal{A}$ depend on both ω and β. Using N sampling points on each edge of Ω_s, u_0 and u_1 are approximated by column vectors of length N, and $\mathcal{A}$ is approximated by a $(2N) \times (2N)$ matrix. A nonzero solution is only possible when $\mathcal{A}$ is singular. This leads to

$$\lambda_1(\mathcal{A}(\omega, \beta)) = 0, \tag{12}$$

where λ_1 is the eigenvalue of $\mathcal{A}$ with the smallest magnitude. Since the real and imaginary parts of λ_1 must vanish simultaneously, the above gives two real equations for the two real unknowns ω and β. When $\mathcal{A}$ is singular, u_0 and u_1 can be solved as the eigenvector corresponding to the eigenvalue $\lambda_1 = 0$. From these two vectors, it is possible to determine u anywhere in the xy plane [42–44].

3. RESULTS

Using the method presented in the previous section, we search BICs for the PhC structure shown in Fig. 1. As in [23], the radius

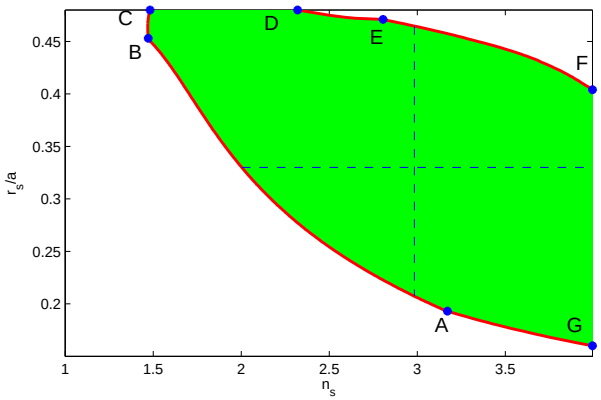

Fig. 2. Existence domain in the $n_s r_s$ plane for a BIC propagating along the surface of the 2D PhC structure shown in Fig. 1, where n_s and r_s are the refractive index and radius of the surface rods.

and dielectric constant of the regular rods are chosen to be $r_1 = 0.2a$ and $\epsilon_1 = 8.9$, but the radius and refractive index of the surface rods are allowed to vary within the bounds given by $r_s \le 0.48a$ and $n_s = \sqrt{\epsilon_s} \le 4$. We obtain a family of BICs that continuously depends on r_s and n_s. Its domain of existence is shown in Fig. 2. Hsu *et al.* [23] first found the BIC for $r_s = 0.33a$ and $\epsilon_s = 8.9$, which corresponds to the intersection point of the two dashed lines in Fig. 2. At this point, the frequency and Bloch wavenumber of the BIC are $\omega a/(2\pi c) = 0.3810$ and $\beta a/(2\pi) = 0.2768$, respectively. The electric field pattern (real part of u) is shown in Fig. 3.

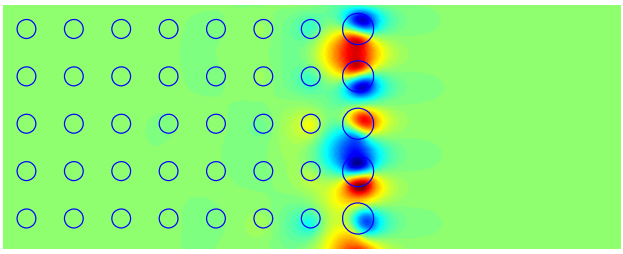

Fig. 3. Electric field pattern (real part of u) of a BIC for the PhC structure shown in Fig. 1 with $r_s = 0.33a$ and $\epsilon_s = 8.9$.

The vertical dashed line shown in Fig. 2 is for $\epsilon_s = 8.9$ and $0.2074 < r_s/a < 0.4646$. Therefore, there is no BIC if the surface rods are identical to the regular ones. Interestingly, the BIC also

ceases to exist if the radius r_s is too large. In Figs. 4(a) and 4(b), we show the frequency and wavenumber of the BIC along the

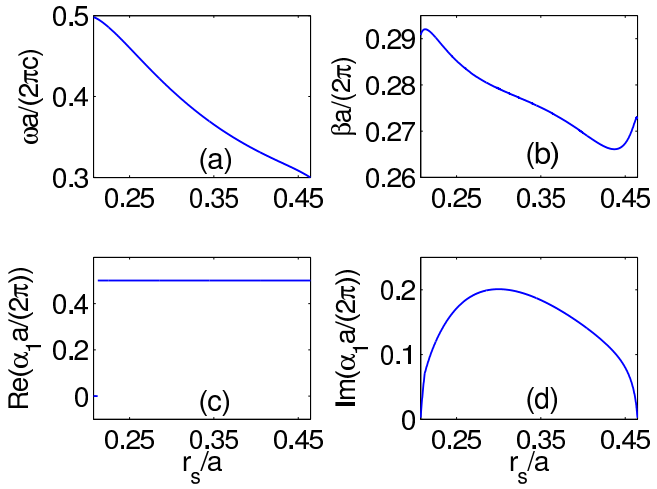

Fig. 4. (a) and (b): Frequency and wavenumber of the BIC as functions of r_s for $\epsilon_s = 8.9$. (c) and (d): Real and imaginary parts of α_1, corresponding to the Bloch mode in the bulk PhC with the slowest decay rate in x.

vertical dashed line as functions of r_s. Figure 4(c) and 4(d) show the real and imaginary parts of α_1 as functions of r_s. Recall that the field of a BIC in the PhC (i.e., for $x < -a/2$) is expanded in Bloch modes as in Eq. (7), where α_j is a wavevector component of the jth Bloch mode, and it is complex with a positive imaginary part. We order the Bloch modes according to the imaginary parts of α_j, with α_1 having the smallest imaginary part. It is clear that $\mathrm{Im}(\alpha_1)$ tends to zero at the two end points of the vertical dashed line, indicating that the field no longer decays in the negative x direction at these two points.

The horizontal dashed line corresponds to $r_s = 0.33a$ and $n_s > 2.003$. In Figs. 5(a) and 5(b), we show the frequency and

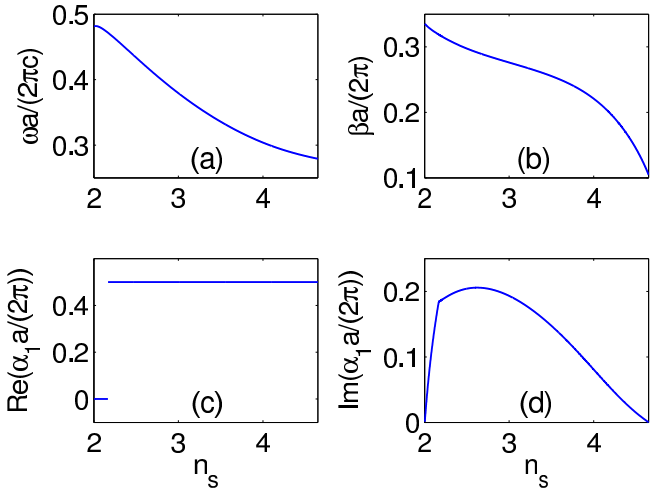

Fig. 5. (a) and (b): Frequency and wavenumber of the BIC as functions of ϵ_s for $r_s = 0.33a$. (c) and (d): Real and imaginary parts of α_1 corresponding to the Bloch mode in the bulk PhC with the slowest decay rate.

wavenumber of the BIC as functions of refractive index n_s. The real and imaginary parts α_1 are shown in Figs. 5(c) and 5(d). As before, $\mathrm{Im}(\alpha_1)$ tends to zero at the two end points. Notice that there is a discontinuity in $\mathrm{Re}(\alpha_1)$ and in the derivative of $\mathrm{Im}(\alpha_1)$. This is caused by two Bloch modes that depend on n_s smoothly and have the same $\mathrm{Im}(\alpha_j)$ at the discontinuity. The definition of our α_1 follows these two different modes in the two sides of the discontinuity, respectively.

It should be emphasized that the domain of existence in Fig. 2 is only for a family of BICs with frequencies between the first and second bands of the bulk PhC. We cannot rule out the possible existence of other BICs inside or outside this domain of existence. For each point in the domain of existence, there is a BIC with a frequency ω and a Bloch wavenumber β. Consequently, there is also a domain in the $\beta\omega$ plane corresponding to the one shown in Fig. 2, and it is the green region shown in Fig. 6. In both Fig. 2 and Fig. 6, we have highlighted seven

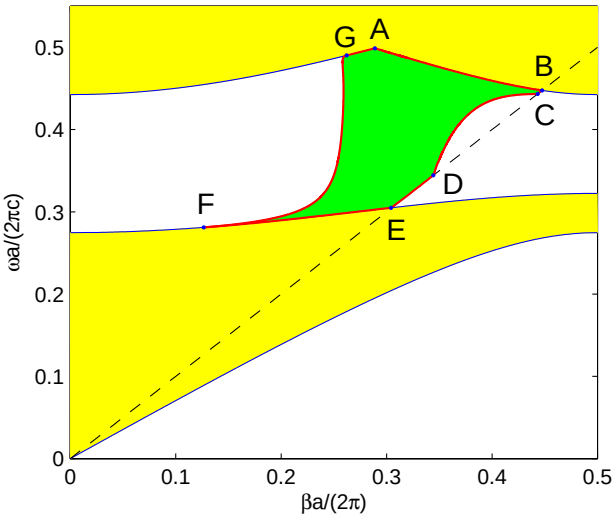

Fig. 6. Projected band structure (yellow regions) of the bulk PhC with rod radius $r_1 = 0.2a$ and dielectric constant $\epsilon_1 = 8.9$, and frequency-wavenumber domain (green region) of the BICs for r_s and ϵ_s shown in Fig. 2.

boundary points by A, B, ..., G. The details of these points are listed in Table 1. In Fig. 6, we also show the projected band

point	n_s	r_s/a	$\beta a/(2\pi)$	$\omega a/(2\pi c)$
A	3.1710	0.1930	0.2888	0.4988
B	1.4720	0.4530	0.4475	0.4476
C	1.4820	0.4800	0.4433	0.4433
D	2.3200	0.4800	0.3444	0.3444
E	2.8060	0.4710	0.3042	0.3049
F	4.0000	0.4032	0.1266	0.2811
G	4.0000	0.1600	0.2620	0.4901

Table 1. Refractive index, radius, Bloch wavenumber and frequency of the seven boundary points A, B, ..., G.

structure of the 2D PhC consisting of the regular rods with radius r_1 and dielectric constant ϵ_1. Bloch waves that propagate in the perfectly periodic PhC are described by their dispersion

surfaces given by $\omega = \omega_j(\alpha, \beta)$, $j = 1, 2, ...$, where (α, β) is the real Bloch wavevector [40]. The two yellow regions are the projections of the first and second dispersion surfaces on the $\beta\omega$ plane, and their boundaries are the extrema of ω_1 and ω_2 with respect to α. It turns out that the minimum and maximum of ω_1 are obtained at $\alpha = 0$ and $\alpha = \pi/a$, respectively. Therefore, the lower and upper boundaries of the first band are given by $\omega = \omega_1(0, \beta)$ and $\omega = \omega_1(\pi/a, \beta)$, respectively. The lower boundary of the second band consists of two pieces separated by point A as shown in Fig. 6, and it is given by

$$\omega = \min_{\alpha} \omega_2(\alpha, \beta) = \begin{cases} \omega_2(\pi/a, \beta), & 0 \le \beta \le \beta_{\mathsf{A}}, \\ \omega_2(0, \beta), & \beta_{\mathsf{A}} < \beta \le \pi/a, \end{cases}$$

where β_{A} is the value of β for point A given in Table 1, i.e., $\beta_{\mathsf{A}} = 0.2888(2\pi/a)$. From Fig. 2 and Fig. 6, it is clear that the existence domain in Fig. 2 is bounded by curves (from A to B, from A to G, and from E to F) related to the band structure of the PhC, and curves (from B to C and from D to E) corresponding to the lightline ($k_0 = \beta$).

As given in Eq. (4), a BIC can be expanded in plane waves with wavevectors (γ_m, β_m) for $x > r_s$. Since the frequency and wavenumber of a BIC are given in the existence domain of Fig. 6, it is clear that $\gamma_0 = (k_0^2 - \beta_0^2)^{1/2}$ is positive, and for $m \neq 0$, $\gamma_m = i(\beta_m^2 - k_0^2)^{1/2}$ is pure imaginary. Since u must decay to zero as x tends to infinity, the coefficient c_0 must vanish. The boundary curves from B to C and from D to E correspond to the lightline $k_0 = \beta$. The BICs can be extended to these boundary curves and the condition $c_0 = 0$ remains valid. In Fig. 7, we

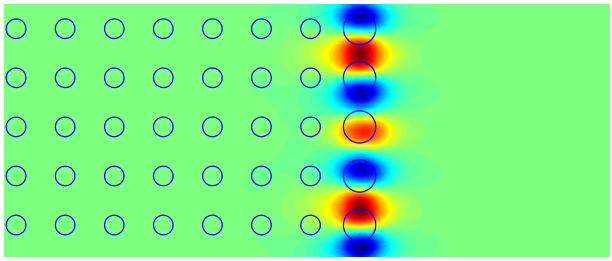

Fig. 7. Electric field pattern (real part of u) of the bound state on the lightline at point D.

show the electric field pattern of the bound state on the lightline at point D.

The above results are obtained with $N = 15$, where N is the number of sampling points on each edge of length a. The operators $\mathcal{P}$ and $\mathcal{L}$ are approximated by 15×15 matrices, Λ is approximated by a 60×60 matrix, and $\mathcal{M}$ and $\mathcal{A}$ are approximated by 30×30 matrices.

4. CONCLUSION

Lightwaves propagating along the surface of a PhC usually exist below the lightline, so that the wave fields are guaranteed to decay in the neighboring free space. Hsu *et al.* [23] first found a propagating Bloch mode above the lightline (i.e. a BIC) on the surface of a 2D PhC consisting of dielectric rods on a square lattice and an array of larger rods at the surface. Unlike the many so-called symmetry-protected BICs, the surface mode of [23] does not have incompatible symmetry with the radiation waves. Although physical arguments and coupled mode models are used to explain the appearance of this and other BICs without symmetry protection [23, 24, 31, 32], it is still not clear why they exist for some values of the structure parameters and do not exist for other values.

In this work, we performed an extensive calculation for BICs at the surface of a 2D PhC. The results reveal that the BICs cease to exist mainly because the bulk PhC can no longer confine light, that is, the frequency and wavenumber of the BIC have reached the boundary of a projected band of the PhC. The other possibility is that the frequency and the wavenumber have reached the lightline. In that case, the BIC ceases to exist only because of its definition. The surface Bloch mode with the key property of the BIC, i.e., $c_0 = 0$ in Eq. (4), exists on and below the lightline. Notice that below the lightline, surface modes exist continuously with respect to the frequency or the wavenumber, but the particular mode with $c_0 = 0$ decays most rapidly in the neighboring free space. Our work is restricted to a particular PhC, but it provides a useful guidance and the necessary background for further studies that may lead to valuable applications.

FUNDING

Fundamental Research Funds for Central Universities of China (Project No. 2015B19614), Research Grants Council of Hong Kong Special Administrative Region, China (CityU 11301914).

APPENDIX A

To derive Eq. (6), we start with the DtN map Λ_1 for unit cell Ω_1 shown in Fig. 1. Let $x_j = (1/2 - j)a$, $u_j(y) = u(x_j, y)$, $v_0(x) = u(x, a/2)$, $v_1(x) = u(x, -a/2)$, then Λ_1 satisfies

$$\Lambda_1 \begin{bmatrix} v_0 \\ u_2 \\ u_1 \\ v_1 \end{bmatrix} = \begin{bmatrix} \partial_y v_0 \\ \partial_x u_2 \\ \partial_x u_1 \\ \partial_y v_1 \end{bmatrix}$$

for $-3a/2 < x < -a/2$ and $-a/2 < y < a/2$, where $\partial_y v_0$ denotes $\partial_y u(x, a/2)$, etc. Since we are concerned with a BIC with Bloch wavenumber β, the quasi-periodic conditions (9) are valid. Therefore, we can eliminate v_0, v_1 and their derivatives, and obtain the operator $\mathcal{M}_1$ satisfying

$$\mathcal{M}_1 \begin{bmatrix} u_2 \\ u_1 \end{bmatrix} = \begin{bmatrix} \mathcal{M}_{11} & \mathcal{M}_{12} \\ \mathcal{M}_{21} & \mathcal{M}_{22} \end{bmatrix} \begin{bmatrix} u_2 \\ u_1 \end{bmatrix} = \begin{bmatrix} \partial_x u_2 \\ \partial_x u_1 \end{bmatrix}. \quad \textbf{(13)}$$

For simplicity, we use the same notations for the blocks of $\mathcal{M}_1$ as those for $\mathcal{M}$ in section 2.

In order to have the expansion (7), we need to solve an eigenvalue problem for the Bloch modes of the bulk PhC. Let $w = \psi(x, y)e^{i(\beta y - \alpha x)}$ be such a mode, where ψ is periodic in both x and y with period a, then

$$w(x_2, y) = \eta w(x_1, y), \quad \partial_x w(x_2, y) = \eta \partial_x w(x_1, y) \quad \textbf{(14)}$$

where $\eta = e^{i\alpha a}$. Equation (13) remains valid when u is replaced by w. From Eqs. (13) and (14), we obtain

$$\begin{bmatrix} \mathcal{M}_{12} & 0 \\ \mathcal{M}_{22} & -I \end{bmatrix} \begin{bmatrix} w(x_1, y) \\ \partial_x w(x_1, y) \end{bmatrix} = \eta \begin{bmatrix} -\mathcal{M}_{11} & I \\ -\mathcal{M}_{21} & 0 \end{bmatrix} \begin{bmatrix} w(x_1, y) \\ \partial_x w(x_1, y) \end{bmatrix}$$

where I is the identity operator. Solving the above eigenvalue problem, we obtain α_k and $w_k(x_1, y)$ for $k = 1, 2, 3, ...$ Since the

eigenvalues appear in pairs, we choose the ones with $\mathrm{Im}(\alpha_k) > 0$. This leads to the Bloch mode expansion (7). If we further define an operator $\mathcal{T}$ such that

$$\mathcal{T} w_k(x_1, y) = e^{i\alpha_k a} w_k(x_1, y), \quad k = 1, 2, 3, \cdots$$

then $\mathcal{T} u_1 = u_2$. Therefore, from Eq. (13), we have

$$\partial_x u_1 = [\mathcal{M}_{22} + \mathcal{M}_{21}\mathcal{T}] u_1.$$

In other words, $\mathcal{L} = \mathcal{M}_{22} + \mathcal{M}_{21}\mathcal{T}$.

REFERENCES

1. C. W. Hsu, B. Zhen, A. D. Stone, J. D. Joannopoulos, and M. Soljačić, "Bound states in the continuum," Nat. Rev. Mater. **1**, 16048 (2016).
2. J. von Neumann and E. Wigner, "Über merkwürdige diskrete eigenwerte," Z. Physik **50**, 291-293 (1929).
3. F. Ursell, "Mathematical aspects of trapping modes in the theory of surface waves," J . Fluid Mech. **183**, 421-437 (1987).
4. D. V. Evans and C. M. Linton, "Trapped modes in open channels," J. Fluid Mech. **225**, 153-175 (1991).
5. J. Goldstone and R. L. Jaffe, "Bound states in twisting tubes," Phys. Rev. B **45**, 14100–14107 (1992).
6. D. V. Evans, M. Levitin and D. Vassiliev, "Existence theorems for trapped modes," J. Fluid Mech. **261**, 21–31 (1994).
7. D. V. Evans and R. Porter, "Trapped modes embedded in the continuous spectrum," Q. J. Mech. Appl. Math. **51**(2), 263–274 (1998).
8. E. N. Bulgakov and A. F. Sadreev, "Bound states in the continuum in photonic waveguides inspired by defects," Phys. Rev. B **78**, 075105 (2008).
9. Y. Plotnik, O. Peleg, F. Dreisow, M. Heinrich, S. Nolte, A. Szameit, and M. Segev,"Experimental observation of optical bound states in the continuum," Phys. Rev. Lett. **107**, 183901 (2011).
10. M. I. Molina, A. E. Miroshnichenko, and Y. S. Kivshar, "Surface bound states in the continuum," Phys. Rev. Lett. **108**, 070401 (2012).
11. S. Weimann, Y. Xu, R. Keil, A. E. Miroshnichenko, A. Tünnermann, S. Nolte, A. A. Sukhorukov, A. Szameit, and Y. S. Kivshar, "Compact surface Fano states embedded in the continuum of the waveguide arrays," Phys. Rev. Lett. **111**, 240403 (2013).
12. C. L. Zou, J.-M. Cui, F.-W. Sun, X. Xiong, X.-B. Zou, Z.-F. Han, and G.-C. Guo, "Guiding light through optical bound states in the continuum for ultrahigh-Q microresonantors," Laser & Photonics Rev. **9**, 114-119 (2015).
13. A.-S. Bonnet-Bendhia and F. Starling, "Guided waves by electromagnetic gratings and nonuniqueness examples for the diffraction problem," Math. Methods Appl. Sci. **17**, 305-338 (1994).
14. P. Paddon and J. F. Young, "Two-dimensional vector-coupled-mode theory for textured planar waveguides," Phys. Rev. B **61**, 2090-2101 (2000).
15. S. G. Tikhodeev, A. L. Yablonskii, E. A Muljarov, N. A. Gippius, and T. Ishihara, "Quasi-guided modes and optical properties of photonic crystal slabs," Phys. Rev. B **66**, 045102 (2002).
16. S. P. Shipman and S. Venakides, "Resonance and bound states in photonic crystal slabs," SIAM J. Appl. Math. **64**, 322-342 (2003).
17. S. Shipman and D. Volkov, "Guided modes in periodic slabs: existence and nonexistence," SIAM J. Appl. Math. **67**, 687–713 (2007).
18. J. Lee, B. Zhen, S. L. Chua, W. Qiu, J. D. Joannopoulos, M. Soljačić, and O. Shapira, "Observation and differentiation of unique high-Q optical resonances near zero wave vector in macroscopic photonic crystal slabs," Phys. Rev. Lett. **109**, 067401 (2012).
19. Z. Hu and Y. Y. Lu, "Standing waves on two-dimensional periodic dielectric waveguides," Journal of Optics **17**, 065601 (2015).
20. R. Porter and D. Evans, "Embedded Rayleigh-Bloch surface waves along periodic rectangular arrays," Wave Motion **43**, 29-50 (2005).
21. D. C. Marinica, A. G. Borisov, and S. V. Shabanov, "Bound states in the continuum in photonics," Phys. Rev. Lett. **100**, 183902 (2008).
22. R. F. Ngangali and S. V. Shabanov, "Electromagnetic bound states in the radiation continuum for periodic double arrays of subwavelength dielectric cylinders," J. Math. Phys. **51**, 102901 (2010).
23. C. W. Hsu, B. Zhen, S.-L. Chua, S. G. Johnson, J. D. Joannopoulos, and M. Soljačić, "Bloch surface eigenstates within the radiation continuum," Light Sci. Appl. **2**, e84 (2013).
24. C. W. Hsu, B. Zhen, J. Lee, S.-L. Chua, S. G. Johnson, J. D. Joannopoulos, and M. Soljačić, "Observation of trapped light within the radiation continuum," Nature **499**, 188–191 (2013).
25. E. N. Bulgakov and A. F. Sadreev, "Bloch bound states in the radiation continuum in a periodic array of dielectric rods," Phys. Rev. A **90**, 053801 (2014).
26. E. N. Bulgakov and A. F. Sadreev, "Light trapping above the light cone in one-dimensional array of dielectric spheres," Phys. Rev. A **92**, 023816 (2015).
27. E. N. Bulgakov and D. N. Maksimov, "Light guiding above the light line in arrays of dielectric nanospheres," Opt. Lett. **41**, 3888 (2016).
28. R. Gansch, S. Kalchmair, P. Genevet, T. Zederbauer, H. Detz, A. M. Andrews, W. Schrenk, F. Capasso, M. Lončar, and G. Strasser, "Measurement of bound states in the continuum by a detector embedded in a photonic crystal," Light: Science & Applications **5**, e16147 (2016).
29. X. Gao, C. W. Hsu, B. Zhen, X. Lin, J. D. Joannopoulos, M. Soljačić, and H. Chen, "Formation mechanism of guided resonances and bound states in the continuum in photonic crystal slabs," Scientific Reports **6**, 31908 (2016).
30. L. Yuan and Y. Y. Lu, "Propagating Bloch modes above the lightline on a periodic array of cylinders," J. Phys. B: Atomic, Mol. and Opt. Phys. **50**, 05LT01 (2017).
31. Y. Yang, C. Peng, Y. Liang, Z. Li, and S. Noda, "Analytical perspective for bound states in the contnuum in photonic crystal slabs," Phys. Rev. Lett. **113**, 037401 (2014).
32. B. Zhen, C. W. Hsu, L. Lu, A. D. Stone, and M. Soljačić, "Topological nature of optical bound states in the contnuum," Phys. Rev. Lett. **113**, 257401 (2014).
33. S. P. Shipman and S. Venakides, "Resonant transmission near nonrobust periodic slab modes," Phys. Rev. E **71**, 02661 (2005).
34. S. Shipman and H. Tu, "Total resonant transmission and refl ection by periodic structures," SIAM J. Appl. Math. **72**, 216-239 (2012).
35. L. Yuan and Y. Y. Lu, "Diffraction of plane waves by a periodic array of nonlinear circular cylinders," Phys. Rev. A **94**, 013852 (2016).
36. L. Yuan and Y. Y. Lu, "Strong resonances on periodic arrays of cylinders and optical bistability with weak incident waves," Phys. Rev. A **95**, 023834 (2017).
37. A. Kodigala, T. Lepetit, Q. Gu, B. Bahari, Y. Fainman, and B. Kanté, "Lasing action from photonic bound states in continuum," Nature **541**, 196-199 (2017).
38. N. Rivera, C. W. Hsu, B. Zhen, H. Buljan, J. D. Joannopoulos, and M. Soljačić, "Controlling directionality and dimensionality of radiation by perturbing separable bound states in the continuum," Sci. Rep. **6**, 33394 (2016).
39. R. D. Meade, K. D. Brommer, A. M. Rappe, and J. D. Joannopoulos, "Electromagnetic Bloch waves at the surface of a photonic crystal," Phys. Rev. B **44**, 10961-10964 (1991).
40. J. D. Joannopoulos, S. G. Johnson, J. N. Winn, and R. D. Meade, Photonic Crystals: Molding the Flow of Light, 2nd ed. (Princeton University Press, Princeton, 2008).
41. K. Ishizaki and S. Noda, "Manipulation of photons at the surface of three-dimensional photonic crystals," Nature **460**, 367-370 (2009).
42. Z. Hu and Y. Y. Lu, "Efficient analysis of photonic crystal devices by Dirichlet-to-Neumann maps," Opt. Express **16**, 17383-17399 (2008).
43. Y. X. Huang and Y. Y. Lu, "Scattering from periodic arrays of cylinders by Dirichlet-to-Neumann maps," J. Lightw. Technol. **24**, 3448-3453 (2006).
44. J. Yuan and Y. Y. Lu, "Photonic bandgap calculations using Dirichlet-to-Neumann maps," J. Opt. Soc. Am. A **23**, 3217-3222 (2006).